ILK is required for the assembly of matrix-forming adhesions and capillary morphogenesis in endothelial cells

Valérie Vouret-Craviari*, Etienne Boulter*, Dominique Grall, Cédric Matthews and Ellen Van Obberghen-Schilling‡

Institute of Signaling, Developmental Biology and Cancer Research CNRS-UMR6543, Centre Antoine Lacassagne, 33 Avenue de Valombrose, 06189 Nice, France

*These authors contributed equally to this work
‡Author for correspondence (e-mail: vanobber@unice.fr)

Accepted 26 May 2004
Journal of Cell Science 117, 4559-4569 Published by The Company of Biologists 2004
doi:10.1242/jcs.01331

Summary

Integrins play a key role in regulating endothelial cell survival, migration and differentiated function during angiogenic blood-vessel remodeling. Integrin-linked kinase (ILK) is a multidomain protein that interacts with the cytoplasmic tail of integrin β subunits and is thought to participate in integrin-mediated signal transduction. We report here that attenuation of ILK expression in cultured bovine aortic endothelial cells by RNA interference had marked effects on surface distribution of α5β1 integrin and the organization of cell-matrix adhesions characterized by the disappearance of fibrillar (3D-like) adhesions that are rich in α5β1 and paxillin, and associated fibrillar fibronectin matrix. This defect was not caused by a decrease in fibronectin mRNA levels or by intracellular retention of the protein. Adhesion to surface-adsorbed matrix proteins based on β1 and β3 integrin was enhanced following ILK depletion, whereas cell spreading, migration and multilayer alignment into capillary-like structures on Matrigel were impaired. We conclude that ILK is an important regulator of the endothelial phenotype and vascular network formation by directing the assembly and/or maturation of α5β1-competent matrix-forming adhesions.

Supplemental data available online at http://jcs.biologists.org/cgi/content/full/117/19/4559/DC1

Key words: Integrin-linked kinase, Endothelial cells, Fibronectin fibrillogenesis, Adhesion, Migration

Introduction

The extracellular matrix plays a determining role in controlling cell survival, proliferation and migration. This regulation takes place largely at the level of clustered integrins, transmembrane receptors that mediate adhesion and activate intracellular signaling modules. Integrins, which lack intrinsic enzymatic activity, transmit intracellular signals by interacting with various effector proteins (Liu et al., 2000). Integrin-linked kinase (ILK) is one such cytoplasmic partner that has recently emerged as an important component of integrin signaling complexes (for reviews, see Dedhar, 2000; Wu and Dedhar, 2001). The protein is composed of distinct domains, including four N-terminal ankyrin repeats followed by a central PH-like sequence and a C-terminal region that is homologous to the catalytic domain of protein kinases. ILK is reportedly involved in several physiological and pathological processes including cell adhesion, E-cadherin expression, fibronectin matrix assembly, transformation and myogenic differentiation (Hannigan et al., 1996; Tan et al., 2001; Wu et al., 1998).

Functional studies of ILK mutants in *Drosophila* (Zervas et al., 2001) and *Caenorhabditis elegans* (Mackinnon et al., 2002) have revealed a crucial role for ILK in linking the actin cytoskeleton and the plasma membrane at sites of integrin-mediated adhesion. More recently, conditional or complete disruption has been reported of the mouse ILK-encoding gene (Grashoff et al., 2003; Sakai et al., 2003; Terpstra et al., 2003). Mice lacking this gene die during early embryonic development owing to a defect in epiblast polarization with an abnormal distribution of F-actin beneath the plasma membrane (Sakai et al., 2003). Chondrocyte-specific disruption of ILK in the mouse leads to chondrodysplasia and respiratory distress causing death of the mice at birth (Grashoff et al., 2003; Terpstra et al., 2003). Cellular defects in ILK-deficient fibroblasts and chondrocytes include impaired adhesion and spreading, altered cytoskeletal organization and a reduced rate of proliferation. Altogether, these findings confirm the key function of ILK as modulator of integrin function.

In cultured mammalian cells, ILK has been localized to cell-matrix adhesion sites by immunofluorescence staining (Li et al., 1999). Several studies have identified ILK interaction with focal adhesion components such as the adaptor protein paxillin, the LIM domain proteins PINCH 1 and 2, the actin-binding proteins CH-ILKBP/actopaxin/α-parvin and β-parvin/affixin (for review, see Wu and Dedhar, 2001), and, more recently, the FERM domain protein UNC-112/mig-2 (Mackinnon et al., 2002). In addition, ILK associates with a serine/threonine protein phosphatase of the PP2C family, referred to as ILKAP (ILK-associated phosphatase) (Leung-Hagesteijn et al., 2001).

The existence of multiple diverse ILK partners suggests that many regulatory mechanisms converge at the level of ILK to mediate integrin signal transduction.

Here, we set out to characterize the role of ILK in regulation of endothelial cell morphology and function by using a specific, effective RNA-interference approach. Our results demonstrate that ILK is an essential cytoplasmic partner of α5β1 integrin required for recruitment of this integrin to fibrillar adhesions and their transformation into competent matrix-forming structures.

Materials and Methods

Materials

All reagents, unless specified, were from Sigma Chemical (Saint Quentin Fallavier, France). Tissue-culture plasticware was from Nunc (Roskilde, Denmark). Sphingosine-1-phosphate (S1P) was from BIOMOL Research (Plymouth Meeting, PA). Collagen type I and human vitronectin were from BD Biosciences (Bedford, MA).

Cell culture

Bovine aortic endothelial cells (BAECs), kindly supplied by H. Drexler (Max-Planck-Institute, Bad Nauheim, Germany), were grown in Dulbecco's modified Eagle's medium (DMEM) with low glucose (Invitrogen Life Technologies, Cergy Pointoise, France) containing 5% heat-inactivated fetal calf serum. For collection of conditioned media, cells (2.5×10^5) were seeded in six-well culture plates 24 hours after the second transfection with RNA duplexes. After 12 hours, cells were washed in serum-free medium for 2 hours then incubated for an additional 24 hours in serum-free medium containing 0.1% bovine serum albumin (BSA). Conditioned medium was harvested, clarified and concentrated tenfold on a Microcon centrifugal filter (10,000 molecular-weight cutoff).

Antibodies

Rabbit polyclonal anti-ILK antibody (DI) was directed against a glutathione-*S*-transferase (GST)-ILK ankyrin-domain fusion protein. Mouse monoclonal anti-ILK (clone 65.1.9) and anti-cortactin (clone 4F11) antibodies were from Upstate Biotechnology (Charlottesville, VA). Anti-AKT and anti-phospho-AKT (pS^{473}) antibody polyclonal antibodies were from Cell Signaling Technology (Beverly, MA). The anti-RhoA monoclonal antibody (clone 26C4) was from Santa Cruz Biotechnology (Santa Cruz, CA) and the monoclonal anti-fibronectin (clone 10) and anti-paxillin (clone 165) antibodies were from BD Biosciences (San Diego, CA). The mouse monoclonal antibody against cyclin D1 (clone DCS-6) was from NeoMarkers (Fremont, CA) and rabbit polyclonal anti-pFAK (pY^{397}) from BioSource International (Nivelles, Belgium). Mouse monoclonal antibodies directed against the integrins αvβ3 (LM609) and α5β1 (HA5), and the rabbit polyclonal anti-α5 integrin antibody were from Chemicon International (Temecula, CA). The rabbit polyclonal anti-ERK antibody (E1B4) that preferentially recognizes ERK2 was raised against a C-terminal ERK1 peptide. Rabbit polyclonal anti-β1 and -β3 antibodies were kindly provided by C. Albiges-Rizzo (Institut Albert Bonniot, Grenoble, France) and N. Kieffer (University Center, Luxembourg), respectively. Anti-phospho-PAK1 polyclonal antibody (Shamah et al., 2001) was a kind gift of S. Shamah and M. Lin (M. Greenberg's laboratory, Harvard Medical School, Boston). Secondary antibodies coupled to horseradish peroxidase or alkaline phosphatase were from Promega France (Charbonnières-les-Bains, France) and New England BioLabs (Beverly, MA), respectively. Fluorescently labeled secondary antibodies were purchased from Molecular Probes (Eugene, OR).

siRNAs and double-stranded RNA transfection

Short interfering RNAs (siRNAs) were purchased from Eurogentec (Serang, Belgium). Equal amounts of complementary RNA oligonucleotides were combined to a final concentration of 20 μM and annealed according to the protocol supplied by the manufacturer. RNA interference in BAECs was achieved by performing two transfections of double-stranded RNA, the first 7 hours after plating and the second 24 hours later, using a modified calcium-phosphate protocol. Unless otherwise stated, cells were analysed between 24 hours and 48 hours after the second transfection. The siRNA sequences used in this study to target ILK (5′-CCCGGCUCA-GGAUUUUCUCTT and 3′-TTGAGAAAAUCCUGAGCCGGG) correspond to a region in the human ILK gene of identical sequence in bovine ILK cDNA (S. Sauze-Fernandez and E.V.O.-S., unpublished). As control, an RNA duplex designed to target the *Drosophila* ILK transcript (GenBank accession number AF226669) was used (5′-CCCAAGCUCCGCAUCUUUUCTT and 3′-TTGAA-AAGTUGCGGAGCUUGGG). The efficiency of ILK silencing, determined by western-blot analyses in each experiment, ranged between 70% and 80%.

Immunofluorescence and deconvolution microscopy

BAECs plated on glass coverslips coated with the indicated matrix protein were fixed in a solution of 3% paraformaldehyde containing 2% sucrose for immunofluorescence staining and mounted in Gel/Mount (Biomedia, Foster City, CA). Fluorescence was observed on a Zeiss inverted microscope (Axiovert 200M) equipped with a CoolSnap HQ cooled charge-coupled-device camera (Roeper Scientifique, Every, France). Image acquisition and analysis was performed using the MetaMorph Imaging System (Universal Imaging Corp.). Deconvolution microscopy using the constrained iterative algorithm (Softworx 2.5, Applied Precision) was performed with the Applied Precision DeltaVision system (Applied Precision, Issaquah, WA) built on an Olympus IX-70 base.

Cell-adhesion assay

The adhesion assay was performed in 96-well microtiter plates coated overnight at 4°C with the indicated doses of matrix proteins or poly-L-lysine, as control. After coating, the wells were washed with PBS and blocked with 0.1% fatty-acid-free BSA in DMEM for 1 hour at 37°C. Cells were detached with trypsin-EDTA, resuspended in serum-free DMEM containing 0.1% fatty-acid-free BSA and plated on the indicated substrates (1.5×10^4 cells per well; 1×10^5 in the case of vitronectin-coated wells). After 40 minutes, non-adherent cells were removed by extensively washing with PBS and remaining cells were fixed and stained with Giemsa. Cell adhesion was determined on triplicate wells by counting attached cells in three different fields. Image analyses were performed using NIH Image software (http://rsb.info.nih.gov/nih-image/default.html). Data are presented as means ± s.e.m.

Migration assays and tube-like structure formation

For the wound healing assay, confluent cells were scraped with a white (10 μl) Gilson pipet tip. Following wounding, the culture medium was changed to remove detached and damaged cells, and wound closure was monitored microscopically 6 hours later. Three different fields of the wound were photographed at the beginning and at the end of the experiment. The wound size was then determined and migration was expressed as the percentage of maximum wound size. Haptotactic migration was analysed on transwell filters (6.5 mm diameter, 8 μM pore size) from Corning (Corning, NY). Trypsinized cells (1.5×10^4) resuspended in DMEM supplemented with 0.1% fatty-acid-free BSA were placed on the upper filter and medium containing chemoattractant filled the lower chamber. After 4 hours, the transwells

were rinsed in PBS to eliminate non-adherent cells and remaining cells in the upper chamber were removed with a cotton bud (Q-Tip®). After an additional wash in PBS, cells were fixed in methanol for 15 minutes at room temperature and stained with 0.1% crystal violet. Three different fields of each transwell were photographed and cells were counted.

Capillary-like structure formation was analyzed on a bed of Matrigel (Beckton Dickinson) (300 μl Matrigel in a 35 mm diameter well). The gel was polymerized at 37°C and 2×10^5 cells in complete Endothelial Growth Medium (PromoCell, Heidelberg, Germany) were seeded on the matrix. Morphological changes were microscopically monitored.

Western blotting and northern analysis

Western blots were performed on whole-cell lysates or conditioned culture medium, separated by SDS-PAGE and transferred to polyvinylidene difluoride membranes (Amersham Pharmacia Biotech, Saclay, France). Proteins were detected by enhanced chemiluminescence using horseradish-peroxidase- or alkaline-phosphatase-based substrates from Pierce (Rockford, IL) and New England BioLabs, respectively. Where indicated, immunoblots were quantified using the GeneGnome chemiluminescent imaging system (Syngene, Frederick, MD). Total RNA was extracted from cells using the Qiagen (Courtaboeuf, France) RNeasy Kit, separated on 1% agarose gels and transferred to hybridization membranes. Polymerase chain reaction (PCR)-generated fragments of the indicated plasmids were radiolabeled using the *redi*prime II random prime kit (Amersham Pharmacia Biotech). Plasmids carrying the wild-type human ILK coding region (1353 bp), the complete wild-type human β1A and the human β3 sequences were kindly provided by S. Dedhar (University of British Colombia, Vancouver, Canada), A. Sonnenberg (The Netherlands Cancer Institute Amsterdam, The Netherlands) and N. Kieffer (University Center, Luxembourg), respectively. A plasmid containing a fragment (fibronectin repeats 6-10) of the human fibronectin cDNA was a gift of K. Yamada (NIH, Bethesda, Maryland, USA).

Fluorescence-activated cell sorting analysis

Surface expression of integrins was determined by flow cytometry using a FACScalibur (Becton Dickinson, Bedford, MA) following detachment of cells. Cells were incubated with anti-αvβ3 (4 μg ml^{-1}) or anti-α5β1 (4 μg ml^{-1}) antibodies for 1 hour at 4°C, rinsed three times with ice-cold PBS and incubated with an anti-mouse antibody coupled to FITC. After three additional washes, cells were fixed with 3.7% formaldehyde and analysed. DNA content was determined according to the protocol provided by Becton Dickinson. Briefly, cells were fixed in ethanol and labeled with propidium iodide (10 μg ml^{-1}) just before the analysis by flow cytometry.

RhoA pull-down assay

Activation of RhoA was measured in a pull-down assay (Ren et al., 1999), as previously described (Vouret-Craviari et al., 2002).

Results

ILK colocalizes with the α5β1 integrin and paxillin in fibrillar adhesions

ILK expression is readily detectable in various cultured endothelial cells from different origins (not shown). Similar to what has been observed in other cell types (Li et al., 1999), endothelial-cell ILK localizes to cell-matrix adhesions. Fluorescent staining of F-actin and ILK in BAECs followed by 3D deconvolution microscopy and digital overlay of images revealed the presence of ILK along the tips of actin microfilaments (Fig. 1, top). Using the same technique, we observed a striking colocalization of ILK and the α5 subunit of the α5β1 fibronectin receptor in these cells (Fig. 1, middle), consistent with the fact that ILK was originally identified as a putative direct ligand for the β1-integrin cytopasmic tail (Hannigan et al., 1996). Co-staining of ILK and α5 was most prominent in fiber-like structures reminiscent of fibrillar adhesions [morphologically defined by Geiger et al. (Geiger et al., 2001)]. Interestingly, immunostaining of paxillin, a focal adhesion

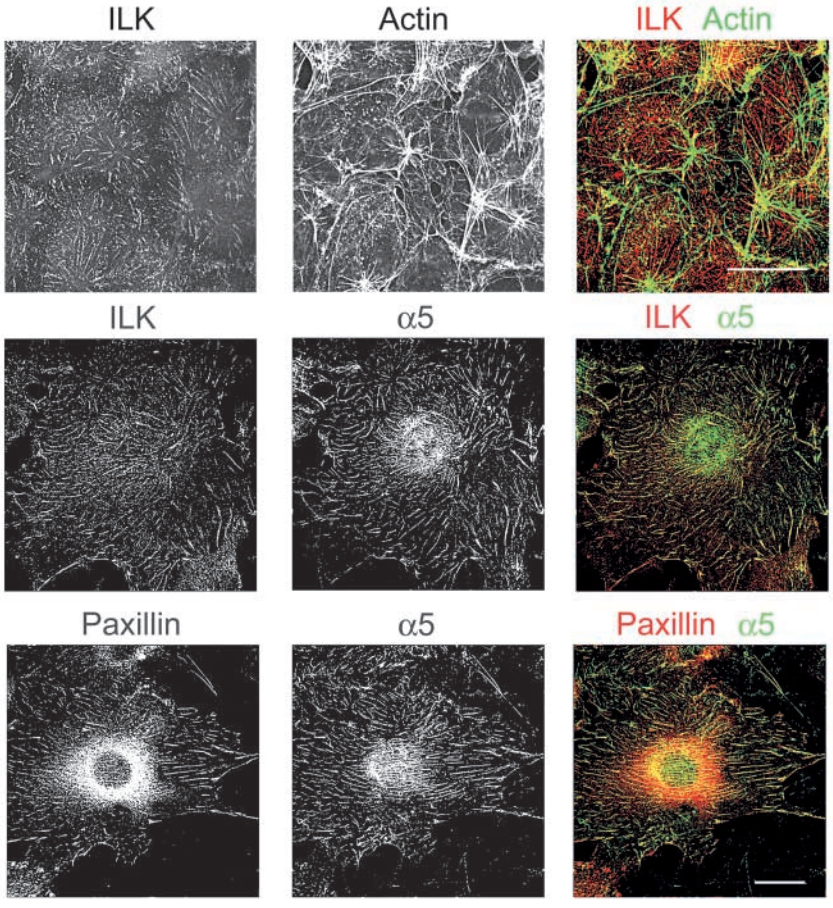

Fig. 1. Subcellular localization of ILK in BAECs. BAECs plated on fibronectin-coated coverslips were fixed, permeabilized and co-stained, as indicated, for F-actin (FITC-phalloidin), ILK (clone 65.1.9), integrin α5 or paxillin (clone 165). Alexa-488-congugated anti-rabbit or Alexa-594-congugated anti-mouse secondary antibodies were used. High-resolution deconvolution microscopy was performed and digital overlays (right) show: (top) co-localization of ILK (red) and F-actin (green) (100×/1.40 plan Apo objective); (middle) ILK (red) and integrin α5 (green); and (bottom) paxillin (red) and integrin α5 (green) (60×/1.40 plan Apo objective). Scale bar, 20 μm.

component reported to interact with ILK (Nikolopoulos and Turner, 2001) also coincided with that of α5 (Fig. 1, bottom), indicating that ILK and paxillin reside in the same α5β1-rich adhesions in these cells. Overlapping localization of paxillin and α5 integrin is a characteristic feature of 3D adhesions or structures formed when cells are attached to 3D fiber meshworks rather than 2D coated surfaces (Cukierman et al., 2002).

Silencing ILK expression in endothelial cells affects cell-matrix adhesions and actin dynamics

To dissect the role of ILK in regulation of endothelial cell adhesion, motility and differentiated function, we used an RNA-interference approach to reduce the expression of the protein selectively in transfected cells. Knock-down experiments were performed in BAECs in which post-transcriptional gene silencing proved to be highly efficient and reproducible. On western blots, ILK migrates as single band of approximately 52 kDa. Transfection of double-stranded RNA molecules complementary to the ILK transcript (ILK siRNA) suppressed ILK expression in these cells by up to 80% compared with control siRNA- or non-transfected cells, as determined by western blotting of cell lysates (Fig. 2A). Northern analysis revealed the total loss of ILK mRNA transcripts under these conditions (Fig. 4C).

Immunofluorescence images confirmed the substantial reduction in ILK levels in ILK siRNA-transfected cells and also revealed differences in the shape of residual ILK-containing structures (Fig. 2B). Whereas ILK staining in control cells highlighted elongated fibrillar adhesions over the entire ventral surface of cells, staining in ILK-deficient cells was restricted to shorter plaques. ILK depletion also had a marked effect on the distribution of paxillin. Thus, the staining of paxillin in fiber-like structures disappeared following ILK suppression and staining became restricted to classical focal adhesions (Fig. 2C). We verified that depletion of ILK did not alter the levels of paxillin expression (data not shown). These findings suggest that ILK might be involved in regulating maturation or turnover of cell-matrix adhesions.

Loss of ILK also incurred changes in the actin-based cytoskeleton characterized by an increase in immunostaining of short, parallel actin stress fibers (Fig. 2C). Under sparse culture conditions, control BAECs extended broad lamellipodial protrusions all around cells, whereas ILK siRNA-transfected cells remained compact and projected structures were smaller (Fig. 2D, top; see supplementary Fig. S1 (http://jcs.biologists.org/cgi/content/full/117/19/4559/DC1)]. Kymograph analyses were performed to examine the effect of ILK depletion on the dynamics of membrane protrusive activity. In the representative kymographs depicted in Fig. 2D, bottom, obtained from phase-contrast time-lapse recordings of cells 2 hours after plating on fibronectin-coated dishes, it can be seen that control cells (left) displayed periodic extension and retraction of lamellipodia. By contrast, the protrusive activity at the edge of ILK-depleted cells (right) remained low. This difference in cell spreading was confirmed by quantitative morphometric analysis of control and ILK siRNA-transfected cells 24 hours after plating on fibronectin-coated coverslips. Indeed, ILK depletion resulted in a twofold reduction in the surface area of spread cells (Fig. 2E). Thus,

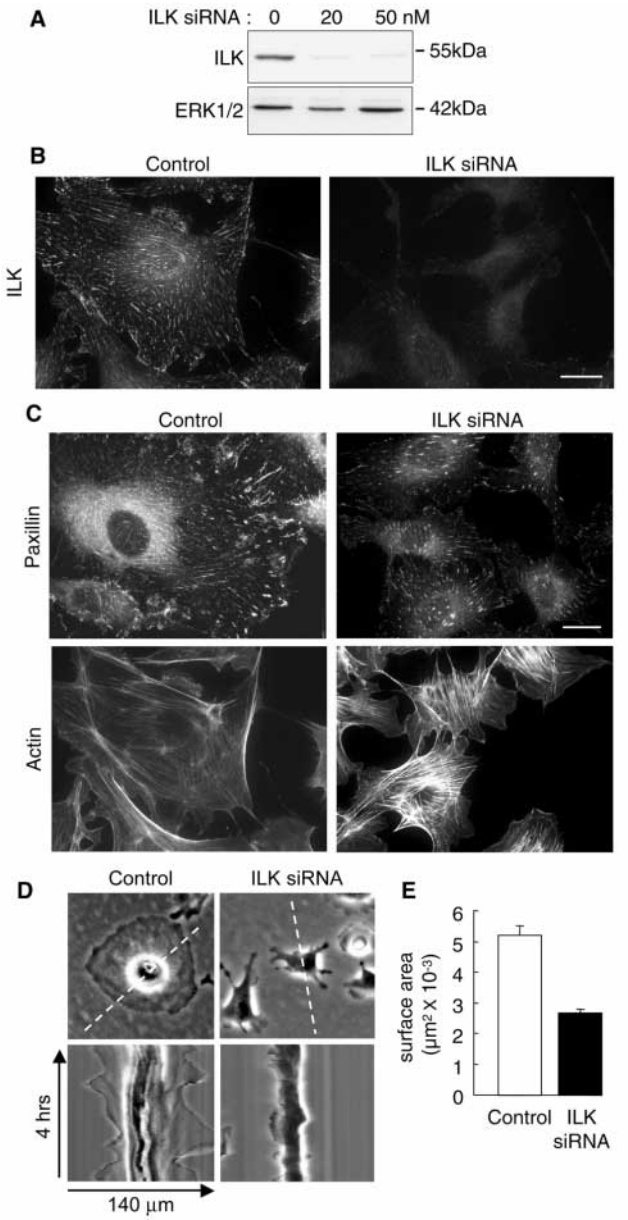

Fig. 2. ILK silencing induces morphological changes in BAECs. BAECs were transfected with the indicated concentration of siRNA duplexes. (A) 48 hours after the second transfection, cells were lysed in Laemmli buffer and ILK expression was analysed by western blotting using a polyclonal anti-ILK antibody (DI). Total ERK1/2 levels were monitored as a control for equal protein loading. (B) Subcellular localization and expression of ILK were determined by immunofluorescence analysis (monoclonal 65.1.9) of cells seeded on fibronectin-coated coverslips 24 hours after the second transfection. A representative photo is shown (scale bar, 20 μm). (C) Cells transfected with control or ILK siRNA were seeded on fibronectin-coated coverslips, fixed and stained with FITC-phalloidin or anti-paxillin antibody (scale bar, 20 μm). (D) Phase-contrast kymograph analysis was performed on time-lapse recordings of control or ILK siRNA-transfected cells using the kymograph function of MetaMorph. Pixel quantification was determined for 4 hours along the rectangle (length, 140 μm) depicted as a dotted line in the phase-contrast images of cells (top). (E) The surface area of spread cells was determined using MetaMorph software on at least 100 F-actin-stained cells from five different fields (100× magnification). Results (means ± s.e.m.) from a representative experiment are shown.

ILK appears to be involved in regulation of molecular events that drive spreading and the extension of membrane protrusions.

ILK silencing alters the distribution of α5β1 integrin and fibronectin matrix assembly

Fibrillar adhesions represent α5β1-rich sites at which integrins bind to fibronectin fibrils and direct matrix assembly. Consistent with a disappearance of these structures in ILK-depleted cells, we noted a striking alteration in the distribution of the α5β1 fibronectin receptor following ILK silencing. Staining of this integrin (visualized with both an anti-α5 polyclonal antibody and an anti-α5β1 monoclonal antibody) appeared largely punctate with occasional localization in small plaque-like structures (Fig. 3). By contrast, ILK silencing had little or no effect on the staining pattern of the vitronectin receptor αvβ3 in cells plated on vitronectin. The αvβ3 integrin is associated with short plaques in both control and ILK siRNA-transfected cells [see supplementary Fig. S2 (http://jcs.biologists.org/cgi/content/full/117/19/4559/DC1)]. Thus, the presence of ILK is required for recruitment of α5β1 into cell-matrix adhesions, whereas it is dispensable for recruitment of αvβ3 to adhesive structures.

The absence of fibrillar adhesions and the perturbed localization of α5β1 in ILK-deficient endothelial cells prompted us to investigate the effect of ILK silencing on fibronectin fibrillogenesis, because α5β1-rich fibrillar adhesions are known to play an important role in this process. Thus, following siRNA transfection, cells were plated on uncoated coverslips for 32 hours before immunostaining without permeabilization for detection of extracellular fibronectin fibrils. In control cultures, a well-defined network of fibrillar fibronectin matrix was associated with most cells (Fig. 4A). By contrast, only weak staining of surface fibronectin could be detected following ILK silencing. To elucidate the mechanism by which ILK silencing impairs fibrillogenesis, we compared the levels of total cellular fibronectin, fibronectin mRNA expression and secretion of the protein in control and ILK siRNA-transfected cells. As shown in Fig. 4A, bottom, immunostaining of fibronectin in permeabilized cells fixed 2.5 hours after plating (to avoid the production of an extensive extracellular fibronectin matrix) revealed that the protein was not preferentially sequestered inside ILK-depleted cells. Thus, the defect in fibrillogenesis in these cells could not be attributed to an intracellular accumulation of fibronectin. An organized extracellular fibronectin matrix could already be detected only 2.5 hours after plating in some control cells, as opposed to ILK siRNA-transfected cells. Accordingly, western blotting showed a dose-dependent decrease in cell-associated fibronectin following ILK siRNA transfection, rather than an augmentation (Fig. 4B). Finally, the levels of fibronectin mRNA were not attenuated in ILK siRNA-transfected cells, excluding the possibility of a suppressive effect of ILK silencing on fibronectin gene transcription or mRNA stability (Fig. 4C). Nonetheless, we did detect a twofold increase in the amount of soluble fibronectin in conditioned medium from ILK-deficient cells (Fig. 4D), consistent with our observation that exogenous fibronectin was unable to rescue this phenotypic trait (not shown). Altogether, these findings support the hypothesis that the defect in fibronectin fibrillogenesis in ILK-depleted cells stems from a deficiency in ILK-dependent fibrillar adhesions.

ILK silencing enhances cell adhesion

We next compared the adhesive properties of control and ILK siRNA-transfected cells. As shown in Fig. 5, reduction of ILK expression had a positive effect on cell adhesion measured 40 minutes after plating. This effect was also observed at earlier times (10 minutes), before spreading occurred (data not shown). Enhanced adhesion of ILK-depleted cells was detected on plates coated with fibronectin, type-I collagen, fibrinogen or vitronectin (Fig. 5). This pleiotypic effect was integrin-dependent, because no significant difference was detected upon adhesion of cells to poly-L-lysine-coated plates, and it was

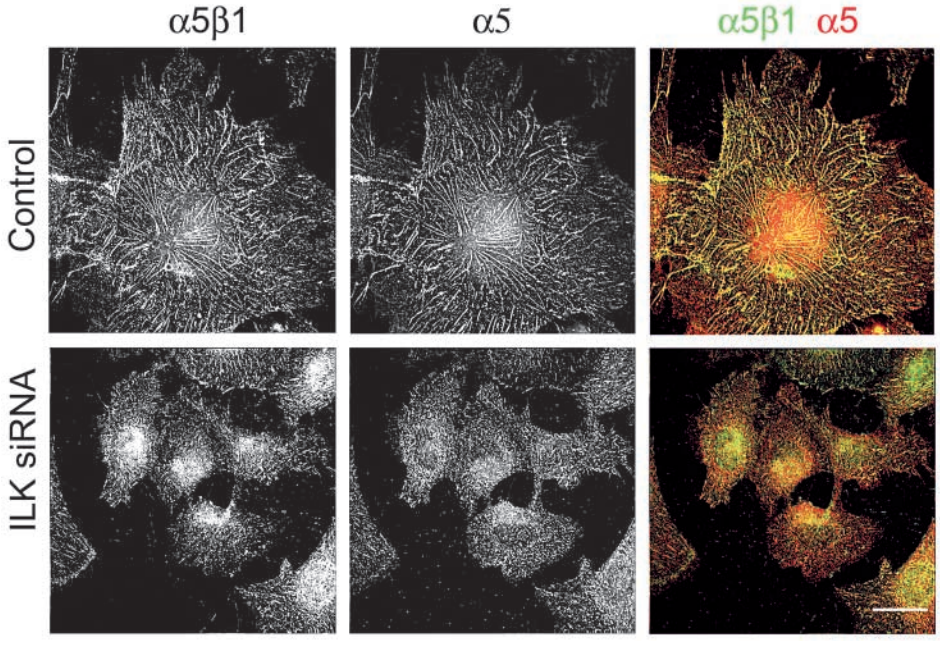

Fig. 3. ILK silencing disorganizes fibrillar adhesions. Surface distribution of the α5β1 integrin in control and ILK siRNA-transfected cells plated on fibronectin-coated coverslips was visualized by co-staining with two different antibodies. Anti-α5β1 monoclonal (HA5, green) detects an extracellular epitope of the heterodimer and anti-α5 polyclonal antibody (red) is directed against a cytoplasmic epitope of the α5 subunit. Alexa-488-congugated anti-mouse and Alexa-594-congugated anti-rabbit secondary antibodies were used; digital overlays of deconvoluted images (60×/1.40 plan Apo objective) are shown on the right. Scale bar, 20 μm.

found at all concentrations of matrix proteins tested (0.1-10 μg ml^{-1}, data not shown). It is noteworthy that ILK-depleted cells were more resistant to detachment than control cells, as quantified using time-lapse images of trypsin-treated cells (data not shown).

Because changes in cell adhesion could simply reflect changes in integrin expression levels, we determined the surface expression of α5β1 and αvβ3 heterodimers on BAEC by fluorescence-activated cell sorting (FACS) analysis. These two fibronectin-binding integrins are of particular importance in vascular development and angiogenesis. Indeed, the specific mean of fluorescence (which corresponds to the increase in fluorescence intensity relative to second antibody alone) was higher for both integrins in ILK-depleted cells (Fig. 6A). This increase was estimated to be 1.86 times for α5β1 and 2.45 times for αvβ3 integrin following ILK siRNA transfection. Total expression of the β1 subunit protein and mRNA was unchanged following ILK silencing, as determined by western blotting of equal amounts of cell lysates, and northern analyses (Fig. 6B,C). Western analysis did reveal a slightly higher level (1.4 times) of the α5 subunit in ILK-deficient cells, which could contribute to the increased surface expression of α5β1 integrin (Fig. 6B). Interestingly, β3 mRNA and protein levels were higher in ILK siRNA-transfected cells than in control cells, indicating that ILK expression can affect β3 transcription and/or mRNA stability differently.

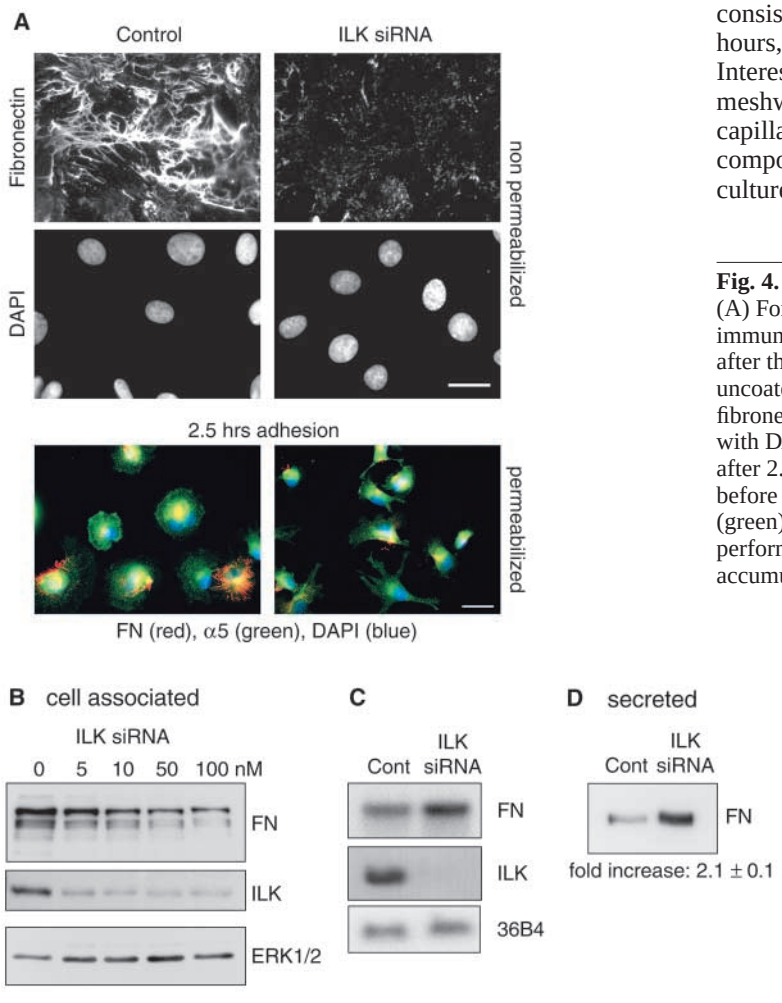

ILK silencing inhibits cell migration and tube-like structure formation

Coordinated regulation of cell adhesion and adhesion complex remodeling are crucial for cell movement. Thus, we sought to evaluate the effect of ILK silencing on BAEC migration. First, an in vitro wound-healing assay was used in which confluent monolayers were disrupted with a pipet tip. After 6 hours, the distance between the parallel migration fronts on either side of the wound was determined at three locations. As shown in Fig. 7A, ILK silencing reduced cell migration into the wound. Whereas the wound size was reduced by 50% in control siRNA-transfected cells, it was reduced by only 10% in ILK-targeted cultures. Decreased cell motility of ILK-depleted cells was confirmed in a modified Boyden-chamber assay. In this case, we observed an inhibition of haptotactic migration through a transwell filter towards fibronectin or collagen (Fig. 7B). Furthermore, following ILK knock-down, cells were insensitive to the chemotactic effect of S1P, a potent stimulator of endothelial cell migration (Fig. 7C).

We next assessed the differentiated phenotype of endothelial cells with reduced ILK expression, as determined by their ability to assume a spindle-shaped morphology and organize into capillary-like structures on a Matrigel basement membrane matrix. Within 6 hours, control siRNA-transfected cells aligned and formed honeycomb structures that became thicker and more homogeneous with time (Fig. 7D). In ILK-deficient cells, this process was significantly delayed, consistent with the observed decrease in their motility. By 20 hours, ILK-depleted cells became organized into a mesh. Interestingly, a striking difference could be seen between the meshwork formed in ILK-deficient and control cultures. The capillary-like structures in ILK-depleted cultures were composed of single-cell alignments, whereas, in control cultures, they were multilayered, as mentioned above. These

Fig. 4. ILK silencing suppresses fibronectin fibrillogenesis. (A) Formation of extracellular fibronectin fibrils was determined by immunostaining of control or ILK siRNA-transfected cells. 24 hours after the second transfection, cells were plated for 32 hours on uncoated glass coverslips before being fixed and stained for fibronectin without permeabilization. (middle) Cell nuclei stained with DAPI (scale bar, 20 μm). (bottom) Merged images of cells fixed after 2.5 hours of adhesion to uncoated coverslips and permeabilized before co-staining for fibronectin (red), the α5 subunit of α5β1 (green) and DAPI (blue). Scale bar, 20 μm. Immunostaining was performed at early times after plating to limit the extracellular accumulation of fibronectin fibrils. (B) 48 hours after the second transfection, cell-associated fibronectin was analysed by western blotting. The same membrane was reblotted for ILK expression to determine the efficiency of ILK silencing in the experiment. Total ERK1/2 levels were analysed as a control for equal protein loading. (C) Northern-blot analysis of fibronectin and ILK mRNA expression in control and ILK siRNA. A probe corresponding to 36B4 (GenBank accession number M17885) was used to control for equal RNA loading. (D) Fibronectin in concentrated 24-hour conditioned medium (corresponding to 250 μl) from control or ILK siRNA-transfected cultures was detected by western blotting. Values below correspond to the fold increase in soluble fibronectin secreted from ILK siRNA-transfected cells relative to control cells (mean ± s.e.m. from three independent experiments).

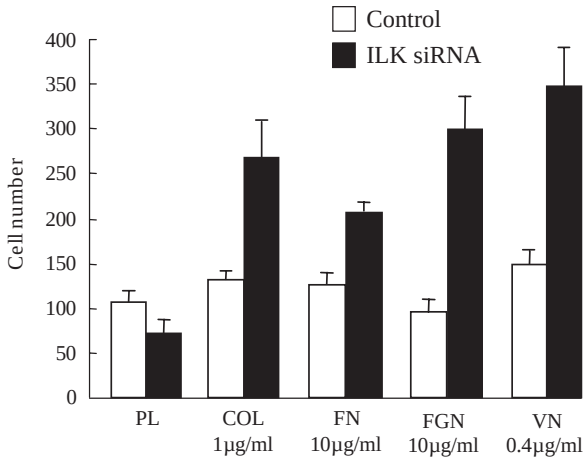

Fig. 5. ILK silencing enhances BAEC adhesion. Control or ILK siRNA-transfected cells were trypsinized, plated on wells coated with the indicated concentration of poly-L-lysine (PL), collagen (COL), fibronectin (FN), fibrinogen (FGN) or vitronectin (VN) and allowed to adhere for 40 minutes. Results represent the number of adherent cells (mean ± s.e.m.) from four independent experiments.

results would suggest that ILK deficiency results in reduced intercellular cohesion on a mixed Matrigel matrix.

Integrin signaling in ILK-deficient cells

RhoA has been found to play a role in the formation of focal adhesions from which stress fibers radiate (Clark et al., 1998; Nobes and Hall, 1995; Rottner et al., 1999) and, more recently, in fibronectin fibrillogenesis (Danen et al., 2002; Zhong et al., 1998). Accordingly, we assessed the possible impact of ILK repression on Rho activity following adhesion of cells to fibronectin-coated plates. The activation status of the GTPase was determined by measuring the levels of GTP-bound RhoA using a pull-down assay. As shown in Fig. 8A, RhoA was activated by adhesion in control siRNA-transfected cells and levels of the GTP-loaded form remained elevated for at least 60 minutes. Thus, 60 minutes after plating, Rho-GTP levels were an average of 2.5 times the basal values (in three independent experiments). In ILK-depleted cells, we observed adhesion-induced RhoA activation, but the extent and persistence of activation was reduced during spreading compared with control cells.

To determine the consequences of ILK silencing on outside-in signaling, we analysed the activation of integrin-stimulated signaling cascades in cells following adhesion. One such cascade involves the protein tyrosine kinase FAK, which is autophosphorylated upon the binding of most integrins to extracellular matrix ligands at a docking site (Tyr-397) involved in recruitment of SH2-containing proteins and activation of the Ras-Raf-ERK cascade (Parsons et al., 2000). Using antibodies that recognize phospho-FAK (pY^{397}), we found no significant difference in the level of FAK phosphorylation between ILK siRNA- and control siRNA-transfected cells following adhesion to fibronectin or collagen (Fig. 8B).

Similar to FAK, no differences were observed in basal or adhesion-stimulated phosphorylation of PAK between control and ILK-depleted cells, as shown in Fig. 8B. Importantly phosphorylation of PAK, a downstream effector of Rac and Cdc42, has previously been shown to reflect changes in Rac1 activity that are below the limits of detection in pull-down assays (Shamah et al., 2001). Thus, by this criterion, ILK silencing does not appear to impair Rac activation. Accordingly, translocation of cortactin from the cytosol to the rim of membrane ruffles in response to S1P, another Rac-dependent event in endothelial cells (Vouret-Craviari et al., 2002), was observed in control and ILK-deficient cells challenged with the agonist (Fig. 8C).

Finally, because ILK has been found to induce phosphorylation of the protein kinases AKT/PKB and GSK3 following adhesion of cells to fibronectin or in response to agonists that activate phosphoinositide-3-kinase, we examined the consequences of ILK silencing on this pathway. As shown in Fig. 9A, we were unable to detect a significant decrease in AKT phosphorylation on Ser-473 in exponentially growing BAECs following ILK siRNA transfection. Further, insulin-stimulated levels of phospho-AKT were comparable in control and ILK siRNA-transfected cells (not shown).

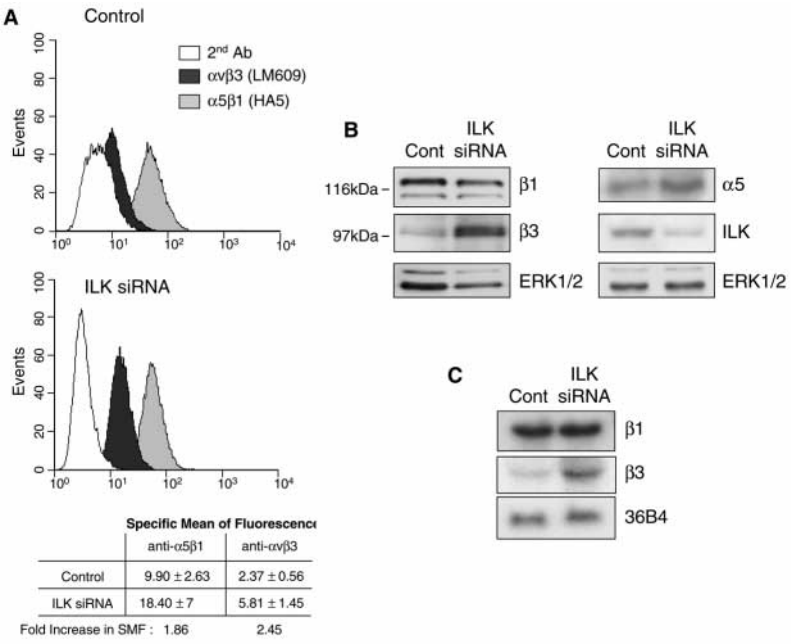

Fig. 6. α5β1 and αvβ3 integrin expression is increased in ILK-depleted cells. (A) Surface integrin expression was measured by flow cytometry. Control or ILK siRNA-transfected cells were labeled with second antibody alone (2^{nd} Ab), anti-α5β1 (HA5) or anti-αvβ3 (LM609). Quantification of specific mean of fluorescence (SMF; which corresponds to the increase in fluorescence intensity relative to second antibody alone) is shown in the table (± s.e.m., n=3 for α5β1 integrin surface expression, n=4 for αvβ3 integrin expression). (B) β1, β3 and α5 integrin subunit expression in control or ILK siRNA-transfected cells was determined by western blotting. Total ERK1/2 levels were monitored as a control for equal protein loading. (C) β1 and β3 integrin mRNA expression was analysed by northern blotting. A probe for 36B4 was used to control for equal loading of RNA.

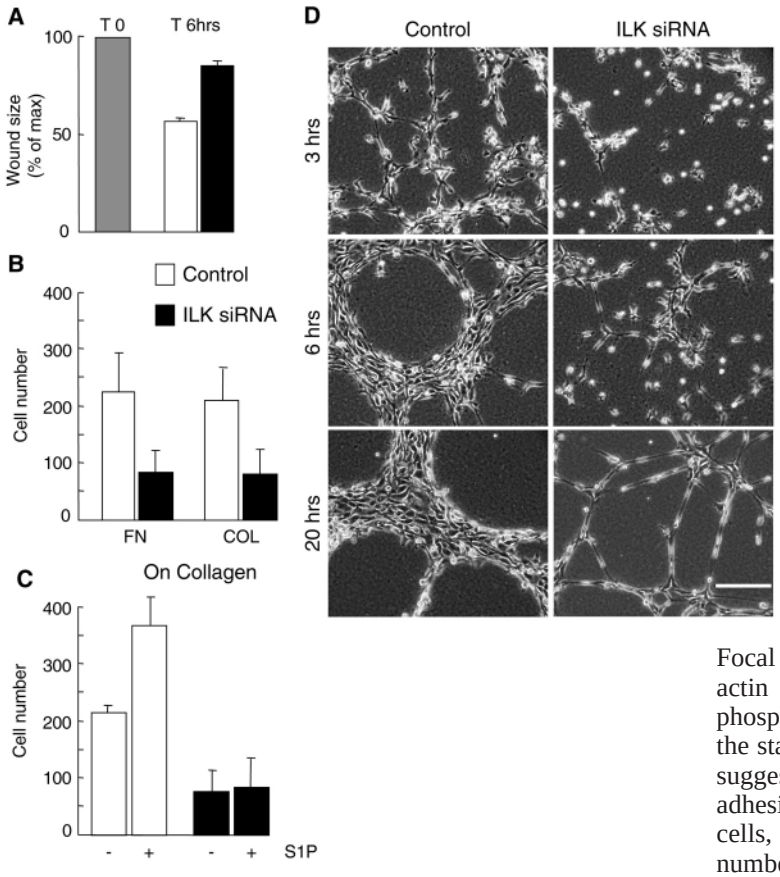

Fig. 7. ILK silencing inhibits BAEC migration and tube-like-structure formation. Migration of control (white bars) or ILK (black bars) siRNA-transfected cells was analysed in a wound-healing assay (A) or in a modified Boyden chamber assay (B,C). (A) At the start of the experiment (T 0), the wound size was scored as 100%. After 6 hours (T 6hrs), cell migration was assayed by measuring the width of the remaining wound. (B) Haptotactic migration was measured in response to 10 μg ml^{-1} fibronectin (FN) or collagen (COL). (C) The chemotactic action of a soluble agonist was determined by placing S1P (1 μM) in the lower chamber. For this experiment, upper and lower chambers were precoated with 10 μg ml^{-1} collagen. (A-C) Mean ± s.d. from two independent experiments. (D) Control or ILK siRNA-transfected cells were plated on a thick Matrigel bed and their ability to form a network of capillary like structures was evaluated. Phase-contrast micrographs (100× magnification) of cells after 3 hours, 6 hours and 20 hours representing three independent experiments. Scale bar, 200 μm.

However, cyclin-D1 expression was suppressed in ILK-deficient cells. Cell-cycle analysis by FACS (Fig. 9B) revealed that this decrease was accompanied by an accumulation of cells in G0/G1 and a decrease in G2/M. It can be seen that sub-G1 DNA content was similar in both control and ILK-depleted cells, indicating that ILK silencing had little or no effect on cell survival.

Discussion

In this study, we set out to characterize the role of ILK in regulation of endothelial cell morphology and function. Because expression of ILK in endothelial cells is relatively high and the endogenous expression levels might not be limiting, we reasoned that overexpression of the protein in these cells might fail to potentiate ILK-dependent processes. Further, because ILK has been found to bind to several partners via distinct domains (for reviews, see Wu, 2001; Wu and Dedhar, 2001), expression of dominant-negative mutants deficient in binding to one or more of these proteins might give partial or misleading results when used to assess certain functions. RNA interference (for review, see Shi, 2003) proved to be an effective way to reduce ILK expression in the endothelial cell model used in the present study. In cultured BAECs, ILK depletion by 80% resulted in several changes in cell morphology and behavior, thus offering new insights into the functions of ILK.

ILK depletion had a marked effect on the formation of cell-matrix adhesions, including focal adhesions and extracellular matrix adhesions, recently renamed fibrillar adhesions (for reviews, see Critchley, 2000; Geiger et al., 2001; Yamada and Geiger, 1997; Zamir and Geiger, 2001). Focal adhesions are typically flat plaques at the tips of actin stress fibers rich in paxillin, vinculin and tyrosine-phosphorylated proteins. ILK depletion in BAECs increased the staining of short paxillin- and vinculin-positive adhesions, suggesting that ILK might be involved in regulating focal-adhesion disassembly or maturation. Similar to ILK-depleted cells, FAK- and Src-deficient cells display an increase in the number of focal adhesions as well as decreased motility. It has been shown that these tyrosine kinases play important roles in the turnover, rather than the assembly of focal adhesions (Ilic et al., 1995; Volberg et al., 2001).

Fibrillar adhesions are elongated structures that arise from focal adhesion and participate in the organization of the extracellular fibronectin matrix. In monolayer cultures, fibrillar adhesions have been shown to contain α5β1 integrin, tensin, α-parvin and little or no phosphotyrosine-containing proteins (Zamir and Geiger, 2001). Under these 2D conditions, paxillin is absent from fibrillar adhesions in fibroblastic cells. However, when cells are cultured in a 3D matrix environment, paxillin has been found to colocalize with α5β1 along fibronectin-containing extracellular fibers in what have been termed 3D-matrix adhesions (for a review, see Cukierman et al., 2002). Interestingly, we found that paxillin colocalizes with α5β1 integrin in fibrillar-type adhesions in control BAECs plated on fibronectin, reminiscent of its localization in 3D-matrix adhesions. Furthermore, ILK (a known paxillin binding partner) is present in these structures. Indeed, 2D cultures of BAECs accumulate an extensive fibronectin network that might mimic a 3D environment. In BAECs, we have not been able to detect the endogenous fibrillar adhesion protein tensin with currently available tools, although molecular characterization of ILK-dependent adhesions in these cells is under way.

Our finding that fibrillar structures are virtually absent from BAECs when ILK expression is suppressed indicates that ILK might participate in the formation of fibrillar adhesions and/or the transformation of focal adhesions into fibrillar adhesions. Although several integrins bind to fibronectin, the principal integrin responsible for fibronectin polymerization is α5β1. This integrin binds soluble fibronectin at the ventral surface in

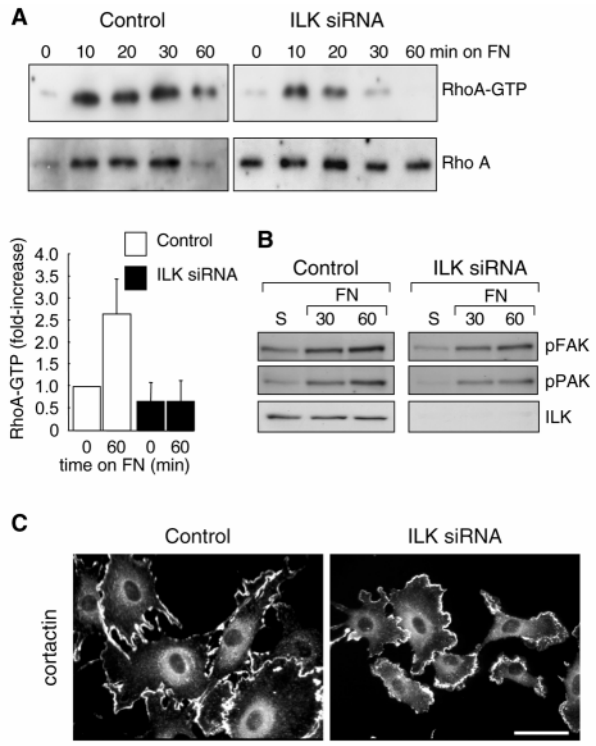

Fig. 8. Effect of ILK silencing on intracellular signaling pathways. (A, top) Activation of RhoA was determined in control or ILK siRNA-transfected cells after adhesion for the indicated times to fibronectin (FN)-coated plates (10 μg ml^{-1}). Quantification of RhoA activation at 60 minutes is shown below; data represent mean values ± s.e.m. from three independent experiments. (B) Activation of FAK and PAK in cells following adhesion of cells to 10 μg ml^{-1} fibronectin (FN) for the indicated time was evaluated by western blotting using anti-pFAK (pY^{397}) and anti-phospho-PAK1 antibodies. (C) Translocation of cortactin to membrane ruffles (a Rac-dependent event) was determined in control and ILK siRNA-transfected cells treated with 0.5 μM sphingosine-1-phosphate (S1P) for 5 minutes by immunostaining with monoclonal anti-cortactin antibody. Scale bar, 40 μm.

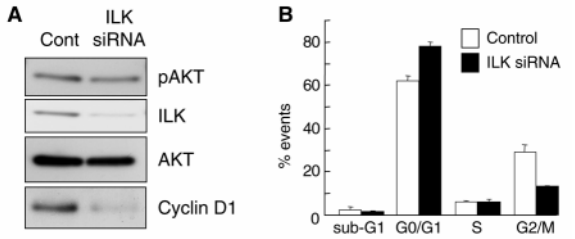

Fig. 9. Effect of ILK silencing on AKT phosphorylation and cell proliferation. (A) The levels of activated AKT and cyclin D1 expression in control and ILK siRNA-transfected cells were determined by western-blot analysis using anti-phospho-AKT (pS^{473}) and anti-cyclin-D1 antibodies, respectively. Total AKT antibody was used to control for equal loading of proteins. (B) Exponentially growing control or ILK-depleted cells were fixed 36 hours after the second transfection and incubated with propidium iodide for analysis of DNA content by FACS. Results are presented as a histogram with mean values (mean ± s.e.m. from three independent experiments) corresponding to the proportion of cells in the indicated phases of the cell cycle.

the case of endothelial cells and, through a cell-driven process involving acto-myosin contractility, cryptic self-assembly sites in the fibronectin molecule are unmasked and spontaneous polymerization occurs. An elegant study of matrix assembly dynamics in human fibroblasts revealed that occupied α5β1 integrin translocates from focal contacts along stress fibers to fibrillar adhesions and this is tightly coupled to fibronectin fibrillogenesis (Pankov et al., 2000). Thus, the fact that ILK is required for association of α5β1 with fibrillar adhesive structures suggests that ILK might be required for this translocation process. Interestingly, ILK-depleted BAECs plated on fibronectin-coated coverslips form α5β1-positive focal adhesions soon after plating. This organization of focal adhesions in ILK siRNA-transfected cells occurs more rapidly than in control cells [see supplementary Fig. S3, 30 minutes after adhesion (http://jcs.biologists.org/cgi/content/full/117/19/4559/DC1)], in accordance with our finding that ILK silencing enhances cell adhesion. However, in absence of ILK, the α5β1-containing plaques disappear within 2-5 hours and staining of the integrin becomes dispersed (Fig. 3, 24 hours after adhesion). Although the mechanisms underlying this phenomenon remain to be elucidated, it is possible that ILK regulates: binding parameters between soluble fibronectin to α5β1; the cell-driven exposure of self-association sites in fibronectin; lateral diffusion and multimerization of the integrin in the membrane; and/or the organization of α5β1-containing adhesion complexes competent for cytoskeletal coupling, a prerequisite for fibronectin matrix assembly. Importantly, we have shown that there is no defect in fibronectin expression or secretion in ILK-deficient cells. Thus, although the absence of ILK does not impair integrin binding to plastic-adsorbed fibronectin (cell adhesion assay), α5β1 is not competent for matrix assembly without ILK-dependent localization to fibrillar adhesions. It is noteworthy that adhesion to fibronectin in both control and ILK-depleted BAECs was mediated by α5β1 integrin, as determined by antibody inhibition assays, whereas adhesion to vitronectin-coated plates occurred via αvβ3 (data not shown). This finding would exclude the possibility that a switch from α5β1- to αvβ3-mediated cell adhesion and spreading accounts for the observed defects in matrix assembly in ILK-depleted cells.

Fibronectin matrix plays important roles in many biological processes including morphogenesis and tumorigenesis. Indeed, a role has been proposed for ILK in fibronectin matrix assembly in epithelial cells (Wu et al., 1998). More recently, ILK overexpression has been implicated in the pathogenesis of diabetic glomerulosclerosis via mesangial matrix expansion (Guo et al., 2001). Our finding that ILK silencing inhibits endothelial cell cohesion in an in vitro tubular morphogenesis assay suggest a new role for ILK-dependent fibronectin matrix deposition in regulation of cellular associations required for vascular network formation. Although the molecular mechanism involved in this process is not known, ILK binding to its partners including PINCH (Tu et al., 1999) and CH-ILKBP (Tu et al., 2001), an actin-binding component of fibrillar adhesions [also known as α-parvin/actopaxin (Nikolopoulos and Turner, 2000; Olski et al., 2001)], is required for localization to cell/extracellular-matrix contacts (Zhang et al., 2002) and fibronectin matrix deposition in mesangial cells (Guo and Wu, 2002).

In light of the observed defects in fibronectin matrix

assembly, it was tempting to speculate that ILK acts by somehow impinging on the Rho pathway. It is noteworthy that robust activation of RhoA by the soluble agonist LPA was observed in both control and ILK siRNA-transfected cells (data not shown). In addition, LPA had similar effects on the actin cytoskeleton in both cell types. Although we did not detect a modification of basal or LPA-stimulated RhoA activity in adherent cells following ILK depletion, we did observe a reduction in the persistence of RhoA activation upon adhesion to fibronectin. The mechanisms responsible for this difference and its implications for adhesion, spreading and fibronectin fibrillogenesis remain to be determined.

Outside-in signaling to FAK was intact following ILK silencing. This finding is not surprising, because vinculin-positive focal adhesions are abundant in ILK-depleted cells. These highly tyrosine-phosphorylated structures containing FAK and downstream signaling components (Parsons et al., 2000) are thought to be the major site of integrin signal transduction. Likewise, the Cdc42/Rac effector PAK is efficiently phosphorylated following adhesion of ILK-depleted cells. In adherent cells, both FAK and PAK are activated in response to serum, independent of ILK expression, and cortactin is translocated to the plasma membrane upon S1P stimulation; this last response is indicative of a functional Rac pathway (Vouret-Craviari et al., 2002). It is noteworthy that, although cortactin translocation takes place in ILK-deficient cells, the projected structures do not have the same morphology [see supplementary Movies 1 and 2 (http://jcs.biologists.org/cgi/content/full/117/19/4559/DC1)]. Thus, in the absence of ILK, some Rac-dependent but ILK-independent events might occur (i.e. cortactin translocation), whereas others (broadening/maturation of lamellipodia) might require both Rac and ILK.

The enhanced adhesion of ILK-depleted endothelial cells to β1 and β3 integrin ligands suggests that, in control cells, ILK might destabilize cell-matrix interactions, at least during the earliest stages of cell adhesion, that were examined in this study. Consistent with this concept, previous studies reported that ILK overexpression significantly impairs cellular adhesion to fibronectin, vitronectin and laminin in epithelial cells (Hannigan et al., 1996), and to collagen matrix in glomerular podocytes (Kretzler et al., 2001). Similarly, in mononuclear leukocytes, overexpression of ILK was found to negatively regulate β1-integrin/VCAM-1-dependent firm adhesion to endothelial cells (Friedrich et al., 2002). The enhanced adhesion observed in ILK-depleted endothelial cells could be attributed to one or more factors including increased integrin expression, modulation of the integrin activation state and/or increased adhesion receptor clustering. At present, our finding that ILK-depleted cells present an increased surface density of α5β1 and αvβ3 offer a possible explanation for this effect. In the case of epithelial cells that manifested impaired adhesion upon ILK overexpression (Hannigan et al., 1996), surface expression of integrins was not altered, and it was suggested that ILK plays a role in inside-out integrin signaling. Indeed a considerable body of evidence indicates that the activation state of integrins is controlled by interaction of their cytoplasmic domains with other proteins that behave as intracellular activators. The ability of ILK to modulate integrin affinity states or to affect integrin aggregation on the plasma membrane, a closely coupled event, remains to be further investigated. It is noteworthy that treatment of ILK-deficient cells with the divalent cation Mn^{2+}, which is known to induce a high-affinity conformation and to mimic integrin activation, increases adhesion to fibronectin similar to control cells (data not shown). From these findings we can conclude that the removal of ILK per se does not confer a pre-activated conformation on fibronectin-binding integrins.

There are certain discrepancies between our findings and the reported cellular defects in deficient fibroblasts and chondrocytes, including impaired adhesion. It is difficult to explain the discrepancies between these findings and our observation that ILK enhances adhesion in endothelial cells following RNA interference. In the reports by Sakai et al. (Sakai et al., 2003), Grashoff et al. (Grashoff et al., 2003) and Terpstra et al. (Terpstra et al., 2003), ILK depletion did not significantly modify integrin expression in cultured cells. It is possible that differences in cellular context (e.g. integrin repertoire and culture conditions) contribute to the divergent effects on cell adhesion. Our findings that ILK-depleted BAECs display reduced cyclin-D1 expression and an increase in G0/G1 arrested cells agree with the findings in ILK-deficient fibroblasts and chondrocytes, although the defect in cell proliferation was only modest in the case of endothelial cells. Further, we did not note any significant decrease in the levels of phospho-AKT present in exponentially growing BAECs following ILK siRNA transfection, consistent with the papers of Sakai and Grashoff (Grashoff et al., 2003; Sakai et al., 2003). For reasons that are presently unclear, these latter results are at variance with reports by Terpstra et al. and Troussard et al. (Terpstra et al., 2003; Troussard et al., 2003).

In conclusion, our work reported here identifies ILK as a key regulator of the endothelial cell phenotype. Further, it provides novel insights into the mechanisms underlying fibrillar adhesion assembly and matrix remodeling that have important implications for integrin function in endothelial network formation.

We thank S. Dedhar, C. Albiges-Rizo, N. Kieffer, S. Shamah, A. Sonnenberg and K. Yamada for providing plasmids and antibodies, and C. Gimond and R. Arkowitz for critical reading of the manuscript and fruitful discussions. These studies were funded by the Centre National de la Recherche Scientifique and the University of Nice (UMR6543), the Association pour la Recherche contre le Cancer and the Association of International Cancer Research. We are indebted to the Emerald Foundation and the Fondation pour la Recherche Médicale for generous support towards the time-lapse and DeltaVision imaging stations, respectively.

References

Clark, E. A., King, W. G., Brugge, J. S., Symons, M. and Hynes, R. O. (1998). Integrin-mediated signals regulated by members of the Rho family of GTPases. *J. Cell Biol.* **142**, 573-586.

Critchley, D. R. (2000). Focal adhesions – the cytoskeletal connection. *Curr. Opin. Cell Biol.* **12**, 133-139.

Cukierman, E., Pankov, R. and Yamada, K. M. (2002). Cell interactions with three-dimensional matrices. *Curr. Opin. Cell Biol.* **14**, 633-639.

Danen, E. H., Sonneveld, P., Brakebusch, C., Fassler, R. and Sonnenberg, A. (2002). The fibronectin-binding integrins alpha5beta1 and alphavbeta3 differentially modulate RhoA-GTP loading, organization of cell matrix adhesions, and fibronectin fibrillogenesis. *J. Cell Biol.* **159**, 1071-1086.

Dedhar, S. (2000). Cell-substrate interactions and signaling through ILK. *Curr. Opin. Cell Biol.* **12**, 250-256.

Friedrich, E. B., Sinha, S., Li, L., Dedhar, S., Force, T., Rosenzweig, A. and Gerszten, R. E. (2002). Role of integrin-linked kinase in leukocyte recruitment. *J. Biol. Chem.* **277**, 16371-16375.

Geiger, B., Bershadsky, A., Pankov, R. and Yamada, K. M. (2001). Transmembrane crosstalk between the extracellular matrix-cytoskeleton crosstalk. *Nat. Rev. Mol. Cell Biol.* **2**, 793-805.

Grashoff, C., Aszodi, A., Sakai, T., Hunziker, E. B. and Fassler, R. (2003). Integrin-linked kinase regulates chondrocyte shape and proliferation. *EMBO Rep.* **4**, 432-438.

Guo, L. and Wu, C. (2002). Regulation of fibronectin matrix deposition and cell proliferation by the PINCH-ILK-CH-ILKBP complex. *FASEB J.* **16**, 1298-1300.

Guo, L., Sanders, P. W., Woods, A. and Wu, C. (2001). The distribution and regulation of integrin-linked kinase in normal and diabetic kidneys. *Am. J. Pathol.* **159**, 1735-1742.

Hannigan, G. E., Leung-Hagesteijn, C., Fitz-Gibbon, L., Coppolino, M. G., Radeva, G., Filmus, J., Bell, J. C. and Dedhar, S. (1996). Regulation of cell adhesion and anchorage-dependent growth by a new beta 1-integrin-linked protein kinase. *Nature* **379**, 91-96.

Ilic, D., Furuta, Y., Kanazawa, S., Takeda, N., Sobue, K., Nakatsuji, N., Nomura, S., Fujimoto, J., Okada, M. and Yamamoto, T. (1995). Reduced cell motility and enhanced focal adhesion contact formation in cells from FAK-deficient mice. *Nature* **377**, 539-544.

Kretzler, M., Teixeira, V. P., Unschuld, P. G., Cohen, C. D., Wanke, R., Edenhofer, I., Mundel, P., Schlondorff, D. and Holthofer, H. (2001). Integrin-linked kinase as a candidate downstream effector in proteinuria. *FASEB J.* **15**, 1843-1845.

Leung-Hagesteijn, C., Mahendra, A., Naruszewicz, I. and Hannigan, G. E. (2001). Modulation of integrin signal transduction by ILKAP, a protein phosphatase 2C associating with the integrin-linked kinase, ILK1. *EMBO J.* **20**, 2160-2170.

Li, F., Zhang, Y. and Wu, C. (1999). Integrin-linked kinase is localized to cell-matrix focal adhesions but not cell-cell adhesion sites and the focal adhesion localization of integrin-linked kinase is regulated by the PINCH-binding ANK repeats. *J. Cell Sci.* **112**, 4589-4599.

Liu, S., Calderwood, D. A. and Ginsberg, M. H. (2000). Integrin cytoplasmic domain-binding proteins. *J. Cell Sci.* **113**, 3563-3571.

Mackinnon, A. C., Qadota, H., Norman, K. R., Moerman, D. G. and Williams, B. D. (2002). *C. elegans* PAT-4/ILK functions as an adaptor protein within integrin adhesion complexes. *Curr. Biol.* **12**, 787-797.

Nikolopoulos, S. N. and Turner, C. E. (2000). Actopaxin, a new focal adhesion protein that binds paxillin LD motifs and actin and regulates cell adhesion. *J. Cell Biol.* **151**, 1435-1448.

Nikolopoulos, S. N. and Turner, C. E. (2001). Integrin-linked kinase (ILK) binding to paxillin LD1 motif regulates ILK localization to focal adhesions. *J. Biol. Chem.* **276**, 23499-23505.

Nobes, C. D. and Hall, A. (1995). Rho, Rac, and Cdc42 GTPases regulate the assembly of multimolecular focal complexes associated with actin stress fibers, lamellipodia, and filopodia. *Cell* **81**, 53-62.

Olski, T. M., Noegel, A. A. and Korenbaum, E. (2001). Parvin, a 42 kDa focal adhesion protein, related to the alpha-actinin superfamily. *J. Cell Sci.* **114**, 525-538.

Pankov, R., Cukierman, E., Katz, B. Z., Matsumoto, K., Lin, D. C., Lin, S., Hahn, C. and Yamada, K. M. (2000). Integrin dynamics and matrix assembly: tensin-dependent translocation of alpha(5)beta(1) integrins promotes early fibronectin fibrillogenesis. *J. Cell Biol.* **148**, 1075-1090.

Parsons, J. T., Martin, K. H., Slack, J. K., Taylor, J. M. and Weed, S. A. (2000). Focal adhesion kinase: a regulator of focal adhesion dynamics and cell movement. *Oncogene* **19**, 5606-5613.

Ren, X. D., Kiosses, W. B. and Schwartz, M. A. (1999). Regulation of the small GTP-binding protein Rho by cell adhesion and the cytoskeleton. *EMBO J.* **18**, 578-585.

Rottner, K., Hall, A. and Small, J. V. (1999). Interplay between Rac and Rho in the control of substrate contact dynamics. *Curr. Biol.* **9**, 640-648.

Sakai, T., Li, S., Docheva, D., Grashoff, C., Sakai, K., Kostka, G., Braun, A., Pfeifer, A., Yurchenco, P. D. and Fassler, R. (2003). Integrin-linked kinase (ILK) is required for polarizing the epiblast, cell adhesion, and controlling actin accumulation. *Genes Dev.* **17**, 926-940.

Shamah, S. M., Lin, M. Z., Goldberg, J. L., Estrach, S., Sahin, M., Hu, L., Bazalakova, M., Neve, R. L., Corfas, G., Debant, A. et al. (2001). EphA receptors regulate growth cone dynamics through the novel guanine nucleotide exchange factor ephexin. *Cell* **105**, 233-244.

Shi, Y. (2003). Mammalian RNAi for the masses. *Trends Genet.* **19**, 9-12.

Tan, C., Costello, P., Sanghera, J., Dominguez, D., Baulida, J., de Herreros, A. G. and Dedhar, S. (2001). Inhibition of integrin linked kinase (ILK) suppresses beta-catenin-Lef/Tcf-dependent transcription and expression of the E-cadherin repressor, snail, in $APC^{-/-}$ human colon carcinoma cells. *Oncogene* **20**, 133-140.

Terpstra, L., Prud'homme, J., Arabian, A., Takeda, S., Karsenty, G., Dedhar, S. and St-Arnaud, R. (2003). Reduced chondrocyte proliferation and chondrodysplasia in mice lacking the integrin-linked kinase in chondrocytes. *J. Cell Biol.* **162**, 139-148.

Troussard, A. A., Mawji, N. N., Ong, C., Mui, A., St Arnaud, R. and Dedhar, S. (2003). Conditional knock-out of integrin-linked kinase (ILK) demonstrates an essential role in PKB/Akt activation. *J. Biol. Chem.* **278**, 22374-22378.

Tu, Y., Li, F., Goicoechea, S. and Wu, C. (1999). The LIM-only protein PINCH directly interacts with integrin-linked kinase and is recruited to integrin-rich sites in spreading cells. *Mol. Cell. Biol.* **19**, 2425-2434.

Tu, Y., Huang, Y., Zhang, Y., Hua, Y. and Wu, C. (2001). A new focal adhesion protein that interacts with integrin-linked kinase and regulates cell adhesion and spreading. *J. Cell Biol.* **153**, 585-598.

Volberg, T., Romer, L., Zamir, E. and Geiger, B. (2001). pp60(c-Src) and related tyrosine kinases: a role in the assembly and reorganization of matrix adhesions. *J. Cell Sci.* **114**, 2279-2289.

Vouret-Craviari, V., Bourcier, C., Boulter, E. and van Obberghen-Schilling, E. (2002). Distinct signals via Rho GTPases and Src drive shape changes by thrombin and sphingosine-1-phosphate in endothelial cells. *J. Cell Sci.* **115**, 2475-2484.

Wu, C. (2001). ILK interactions. *J. Cell Sci.* **114**, 2549-2550.

Wu, C. and Dedhar, S. (2001). Integrin-linked kinase (ILK) and its interactors: a new paradigm for the coupling of extracellular matrix to actin cytoskeleton and signaling complexes. *J. Cell Biol.* **155**, 505-510.

Wu, C., Keightley, S. Y., Leung-Hagesteijn, C., Radeva, G., Coppolino, M., Goicoechea, S., McDonald, J. A. and Dedhar, S. (1998). Integrin-linked protein kinase regulates fibronectin matrix assembly, E-cadherin expression, and tumorigenicity. *J. Biol. Chem.* **273**, 528-536.

Yamada, K. M. and Geiger, B. (1997). Molecular interactions in cell adhesion complexes. *Curr. Opin. Cell Biol.* **9**, 76-85.

Zamir, E. and Geiger, B. (2001). Molecular complexity and dynamics of cell-matrix adhesions. *J. Cell Sci.* **114**, 3583-3590.

Zervas, C. G., Gregory, S. L. and Brown, N. H. (2001). *Drosophila* integrin-linked kinase is required at sites of integrin adhesion to link the cytoskeleton to the plasma membrane. *J. Cell Biol.* **152**, 1007-1018.

Zhang, Y., Chen, K., Tu, Y., Velyvis, A., Yang, Y., Qin, J. and Wu, C. (2002). Assembly of the PINCH-ILK-CH-ILKBP complex precedes and is essential for localization of each component to cell-matrix adhesion sites. *J. Cell Sci.* **115**, 4777-4786.

Zhong, C., Chrzanowska-Wodnicka, M., Brown, J., Shaub, A., Belkin, A. M. and Burridge, K. (1998). Rho-mediated contractility exposes a cryptic site in fibronectin and induces fibronectin matrix assembly. *J. Cell Biol.* **141**, 539-551.